

# High-efficiency $\sim 2$ $\mu\text{m}$ laser in a single-mode Tm-doped lead germanate composite fiber

Peiwen Kuan (关珮雯)<sup>1,2</sup>, Xiaokang Fan (范小康)<sup>3</sup>, Wentao Li (李文涛)<sup>1,2</sup>,  
Xueqiang Liu (刘雪强)<sup>1,2</sup>, Chunlei Yu (于春雷)<sup>1</sup>, Lei Zhang (张磊)<sup>1</sup>, and  
Lili Hu (胡丽丽)<sup>1,\*</sup>

<sup>1</sup>Key Laboratory of Materials for High Power Laser, Shanghai Institute of Optics and Fine Mechanics,  
Chinese Academy of Sciences, Shanghai 201800, China

<sup>2</sup>University of Chinese Academy of Sciences, Beijing 100039, China

<sup>3</sup>Wuhan Optics Valley Aerospace Sanjiang Laser Industrial Technology Research Institute Co. Ltd.,  
Wuhan 430000, China

\*Corresponding author: leizhju@siom.ac.cn

Received April 13, 2016; accepted June 14, 2016; posted online July 20, 2016

A highly Tm-doped lead germanate glass fiber is developed using the rod-in-tube method. The  $\sim 2$   $\mu\text{m}$  laser beam quality of the fiber is  $\sim 1.5$ . The lead germanate composite fiber jumpers are homemade for all the fiber laser investigations. When core is pumped by a 1590 nm Yb/Er fiber laser, a maximum laser output of 313 mW is achieved at a 670 mW pump power, and the corresponding slope efficiency is  $\sim 52.8\%$ . Moreover, by using a 2 cm-long lead germanate fiber as the gain medium, a 33 mW 1942 nm Tm laser is also demonstrated.

OCIS codes: 160.5690, 160.2290, 140.3510.

doi: 10.3788/COL201614.081601.

Fiber lasers operating in the 2  $\mu\text{m}$  eye-safe region have been studied extensively owing to their potential applications, including environmental sensing, laser radar, space communication, and efficient mid-infrared (IR) light generation<sup>[1-3]</sup>. In the past decade, rapid progress has been made with the development of  $\sim 2$   $\mu\text{m}$  Tm-doped fiber lasers. Compared with silica glass, multicomponent glass as a fiber host has several advantages, including a lower phonon energy, resulting in a wider IR transmission range, high rare earth solubility, resulting in high gain per unit length, and a larger absorption/emission cross section, and it has attracted considerable attention<sup>[4-9]</sup>. In particular, germanate glasses, which have not only better mechanical strength and chemical durability than fluoride glasses but also higher thermal stability than tellurite glasses for output scaling, are promising materials for realizing 2  $\mu\text{m}$  fiber lasers. In 2007, a 104 W  $\sim 2$   $\mu\text{m}$  laser produced by a large-core-area single-mode germanate fiber was reported<sup>[10]</sup>, and it is the highest output power among various multicomponent glass fibers. Furthermore, some efforts for developing germanate fiber glasses have also been made. For example, a 0.75 W laser output with a slope efficiency of 28.7% was obtained in a Tm-doped tellurium germanate glass fiber pumped by a 793 nm diode laser<sup>[11]</sup>. With an in-band pump at 1568 nm, an  $\sim 2$ - $\mu\text{m}$  Tm-doped fiber laser in a barium gallo-germanate glass system was demonstrated with a slope efficiency of 7.6%<sup>[12]</sup>.

In comparison, lead germanate glass systems have relatively large glass-forming regions, low softening temperatures, and good formability while maintaining high IR transmissions<sup>[13-15]</sup>, which make them potential candidates for mid-IR fibers. A Tm-doped lead germanate fiber laser at 1.88  $\mu\text{m}$ , pumped by a 794-nm Ti:sapphire laser and

with a slope efficiency of 13%, was first reported in 1992<sup>[16]</sup>. In our previous work<sup>[17]</sup>, we demonstrated an  $\sim 2$   $\mu\text{m}$  continuous-wave laser and a passively pulsed laser based on a lead germanate fiber. Commercial lead silicate glasses, which possess the appropriate thermal properties and viscosities, can be used as fiber cladding materials to reduce the cost. In these reports, the large difference between the refractive indices of the germanate glass core and the silicate glass cladding leads to a multimode laser operation. However, a single-mode fiber is needed for developing laser oscillators, such as single frequency and ultra-fast fiber lasers. Furthermore, the different glass materials of the core and cladding might form an unsatisfactory interface during fiber drawing, which may depress the fiber laser performance.

In this work, a newly Tm-doped lead germanate double-cladding composite fiber was developed. Silicate glass was used as the outer cladding, and the fiber core and the inner cladding were both made of lead germanate glass. The  $\sim 2$   $\mu\text{m}$  laser beam quality of the fiber was measured as  $\sim 1.5$ . Under pump of a 1590 nm laser, a maximum  $\sim 2$   $\mu\text{m}$  laser output of 313 mW was obtained in an all-fiber configuration, and the corresponding slope efficiency was  $\sim 52.8\%$ . Moreover, in a short fiber length of 2 cm, an unsaturated 33 mW 1940 nm laser was achieved.

Using the same glass composition (50GeO<sub>2</sub>-5SiO<sub>2</sub>-20PbO-20CaO-5K<sub>2</sub>O) for the core and inner-cladding guarantees a high-quality interface. The  $3.1 \times 10^{20}$ -ions/cm<sup>3</sup> Tm-doped core glass and the inner-cladding glass were prepared by a conventional quenching method. The well-mixed 300 g batches were first heated in a vacuum drying oven at 200°C for 48 h to remove the crystal water content in the raw materials, and then they were melted

in a platinum crucible at  $\sim 1200^\circ\text{C}$  for 3 h. After 3 h, dried  $\text{O}_2$  was bubbled into the glass melt for 1 h to eliminate the  $\text{OH}^-$  groups. The melts were then casted on a preheated stainless steel mold and annealed in a muffle furnace at  $\sim 500^\circ\text{C}$  for 100 h. The entire preparation process was conducted in a dried environment (relative humidity  $\leq 5\%$  at  $18^\circ\text{C}$ ).

A commercial lead silicate glass (CDGM Glass Co., Ltd) used for the outer cladding can improve the fiber robustness and reduce the cost. The thermal properties of all three glasses are listed in Table 1; no crystallization ( $T_x = \text{N/A}$ ) indicates that the glass has good thermal stability for fiber fabrication. The IR transmission spectrum of a 0.5 mm-thick core glass sample, the cutoff edges of which can be up to  $\sim 6 \mu\text{m}$ , is shown in Fig. 1. The core glass had an estimated  $\text{OH}^-$  absorption coefficient of  $0.45 \text{ cm}^{-1}$ . The relatively low OH content leads to a long lifetime for the  $^3\text{F}_4$  level of  $\text{Tm}^{3+}$ , which is measured to be  $2041 \mu\text{s}$  in the bulk core glass. In contrast to the Tm-doped silica fiber<sup>[1]</sup>, the longer lifetime is beneficial to the population of the upper lasing level. The maximum simulated emission cross section at 1864 nm, calculated with the Fuchtbauer-Ladenburg formula<sup>[18,19]</sup>, was  $6.15 \times 10^{-21} \text{ cm}^2$ , which is larger than that in silicate glasses ( $3.59 \times 10^{-21} \text{ cm}^2$ )<sup>[20]</sup> and ZBLAN glass ( $2.31 \times 10^{-21} \text{ cm}^2$ )<sup>[21]</sup>, as shown in Fig. 2.

The Tm-doped lead germanate glass fiber (TLGF) was designed to match the conventional silica fiber and fabricated in house using the rod-in-tube technique. The fiber had a  $7.8 \mu\text{m}$ -diameter core with an NA of 0.156 and a  $24 \mu\text{m}$ -diameter circular inner cladding with an NA of 0.31. The diameter of the fiber was  $125 \mu\text{m}$ . Although the size and NA value of the fiber core were slightly different from that of the commercial fiber (Corning SMF-28e), the measured insertion loss between the two fibers in our experiment was less than 1 dB. The index curve with respect to the wavelength was fitted according to the Sellmeier equation. The single-mode cutoff wavelength of the composite fiber is  $\sim 1.59 \mu\text{m}$ , and thereby the fiber supports single transverse-mode  $2 \mu\text{m}$ -laser operation. The propagation loss of the fiber at  $1310 \text{ nm}$  was measured to be  $\sim 0.022 \text{ dB/cm}$ , which was 30% less than the value in our previous work<sup>[17]</sup>, and only half that of  $\text{Tm}^{3+}$ -doped barium gallo-germanate glass fiber ( $0.05 \text{ dB/cm}$ )<sup>[12]</sup>. This improvement can be mainly ascribed to the homogeneous

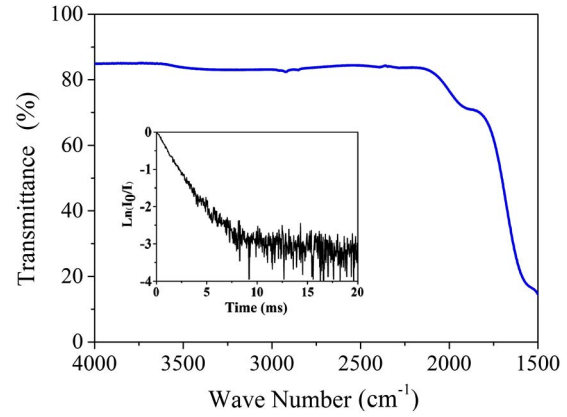


Fig. 1. IR transmission spectrum of germanate core glass. The inset shows the fluorescence decay curve of the  $^3\text{F}_4$  level.

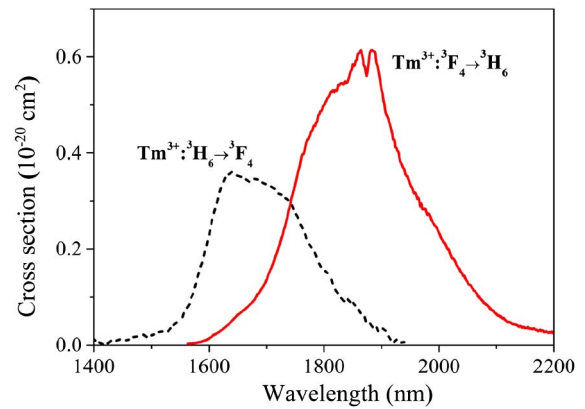


Fig. 2. Absorption and emission cross sections of  $\text{Tm}^{3+} : ^3\text{H}_6 - ^3\text{F}_4$  transition.

material utilized for the core and cladding. Using a beam profiler (Thorlabs), the laser beam quality from a Tm-doped lead germanate composite fiber laser was clarified as well, as shown in Fig. 3. In the measurement, the Tm-doped composite fiber was spatially pumped by a  $792 \text{ nm}$  laser diode. After the pump filter, the output laser was directly coupled from the TLGF and has a central wavelength of  $1889 \text{ nm}$ . The  $M^2$  factor of the laser was measured to be  $\sim 1.5$ , confirming a moderate beam quality from the single-mode composite fiber. The laser beam profile inserted in Fig. 3(b) was a Gaussian distribution.

**Table 1.** Thermal Properties of Bulk Glasses and Fiber Parameters

	Glass	$T_g$ ( $^\circ\text{C}$ )	$T_x$ ( $^\circ\text{C}$ )	CTE ( $10^{-6}/^\circ\text{C}$ )	Diameter ( $\mu\text{m}$ )	Refractive index @1552 nm	NA
Active core	Germanate	472.6	N/A	9.9752	7.8	1.77923	0.156
Inner cladding	Germanate	475.2	N/A	N/A	24	1.77239	0.310
Outer cladding	Silicate	425.8	N/A	9.479	125	1.74504	

( $T_g$ , glass transition temperature;  $T_x$ , onset temperature of crystallization; CTE, coefficient of thermal expansion at  $30^\circ\text{C}$ – $300^\circ\text{C}$ ).

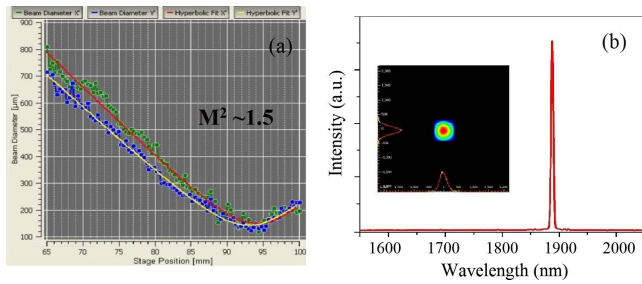


Fig. 3. (a) The beam quality measurement of a Tm-doped composite fiber laser at 200 mW. (b) The corresponding laser profile and laser spectrum.

In-band/tandem pumping is becoming a popular scheme for exciting Tm<sup>3+</sup> ions owing to its high Stokes efficiency, low quantum defect, and low thermal loading, opening the prospect of high lasing efficiency and the potential for further power scaling<sup>[8,22–24]</sup>. Thus, in this work, an Yb/Er co-doped single-mode fiber laser operating at 1590 nm was employed as the pump source. By an efficient core-pump scheme, the  $\sim 2$   $\mu$ m Tm-doped fiber laser performance was investigated. The measured absorption of TLGF at 1590 nm was  $\sim 50 \pm 5$  dB/m. The homemade lead germanate fiber jumpers were used to connect the lead germanate fiber and the silica fiber in a flange to form a stable and simple all-fiber laser configuration. The experimental setup is shown in Fig. 4. The linear laser oscillator comprises a TLGF, a high-reflection (HR) mirror (>99.9%) at  $\sim 2$   $\mu$ m, and a wavelength division multiplexer. The perpendicular cleaved output end, the Fresnel reflection of which is  $\sim 4\%$ , was used as an output coupler. The lead germanate fiber jumpers, 19, 39, and 55 cm long, were prepared as the gain medium for the laser cavity.

The  $\sim 2$   $\mu$ m laser output power was recorded as a function of the incident pump power, and the results at different fiber lengths were investigated, as shown in Fig. 5. The slope efficiencies of the  $\sim 2$   $\mu$ m laser of fiber lengths 19, 39, and 55 cm were about 52.8%, 54.9%, and 53.5%, respectively. No pump saturation was observed when the incident power was less than 700 mW, indicating that a higher output power could be obtained by enhancing the pump power. Figure 5(a) shows that the slope efficiency slightly varies depending on the TLGF length. The highest slope efficiency of the three fibers, i.e., 54.9%,

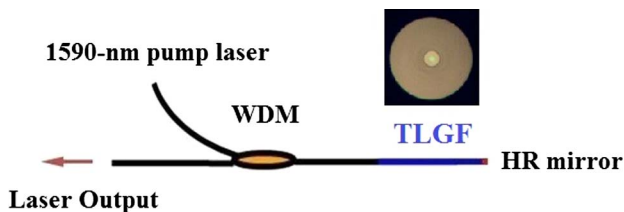


Fig. 4. Experimental setup of a Tm-doped lead germanate composite fiber laser pumped by a 1590 nm laser. The fiber cross section is a polished TLGF pigtail.

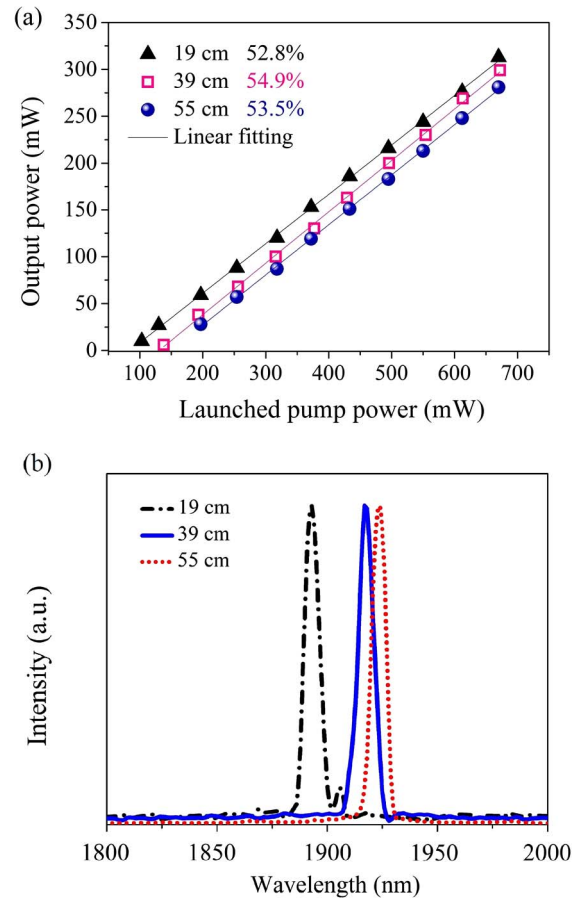


Fig. 5. (a) Laser output power versus 1590 nm launched pump power and (b) normalized laser spectra for different TLGF lengths.

which was exhibited in the 39 cm-long fiber, can be attributed to the suitable pump absorption of  $\sim 17.7$  dB. The 19 cm-long fiber could not make the best use of the incident pump power, but it did have less background loss. Thus, its laser threshold was lower than that of the 39 and 55 cm-long fibers, and its maximum output power was 313 mW at a launched pump power of 670 mW. Figure 5(b) presents the laser spectra of the TLGF lasers of various fiber lengths. As the fiber length increases, the peak wavelength of the laser becomes longer (from 1893 to 1924 nm) due to radiation trapping. Compared with the single-cladding composite fiber<sup>[17,25]</sup>, a significant improvement of the  $\sim 2$   $\mu$ m laser was seen in our results.

In addition, a 2 cm-long TLGF for laser output was also demonstrated. The laser cavity was constructed by the HR mirror and a 1942 nm fiber Bragg grating (FBG) (with 65% reflection and a 0.3 nm bandwidth). The laser output was recorded with respect to the launched pump power, as shown in Fig. 6(a). The laser spectrum was measured by an optical spectrum analyzer with an optical resolution of 0.05 nm. The peak wavelength at  $\sim 1942.3$  nm matched the FBG and had a 3 dB bandwidth of  $\sim 0.14$  nm. The laser threshold of the launched pump power was  $\sim 94$  mW, which corresponds to an absorbed pump power of 23 mW.

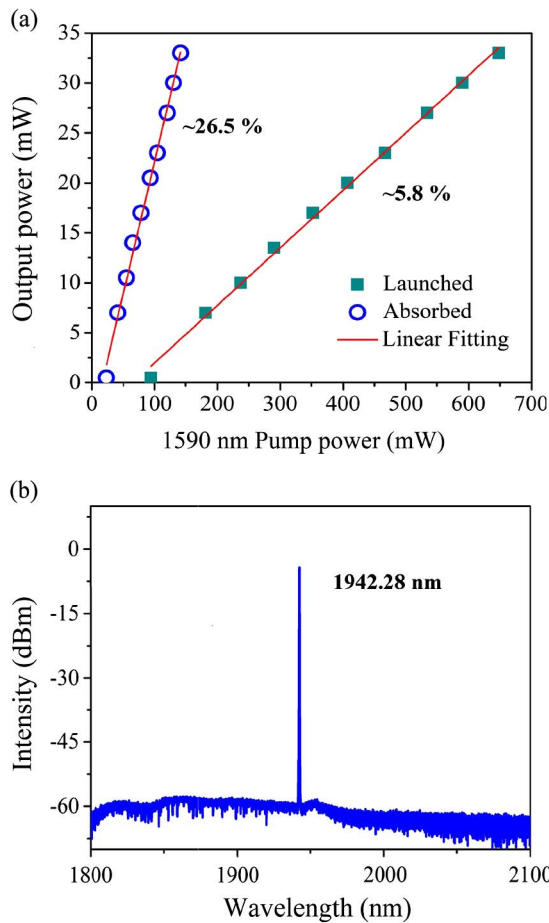


Fig. 6. (a) Laser output and (b) laser spectrum from a 2 cm TLGF laser.

The maximum output power of 33 mW was obtained at a pump power of 648 mW. The slope efficiencies of the 2 cm-long TLGF laser with respect to the launched and the absorbed pump powers were 5.8% and 26.5%, respectively. Such a compact fiber laser shows great promise for single-frequency laser operation.

In conclusion, we design and fabricate a single-mode TLGF. Improving the fiber quality, an efficient  $\sim 2$   $\mu\text{m}$  single-mode laser is demonstrated. With an in-band 1590 nm pump source, a high slope efficiency of  $\sim 54.9\%$  is achieved in a 39 cm-long TLGF, and a maximum  $\sim 2$   $\mu\text{m}$  laser output of 313 mW is realized in a 19 cm-long TLGF at a pump power of 670 mW. Furthermore, in a 2 cm-long fiber, a 33 mW 1942 nm laser is demonstrated. These results indicate that this fiber has great potential for 2  $\mu\text{m}$  single-frequency fiber lasers or high-repetition-rate mode-locked fiber lasers.

This work was supported by the National Natural Science Foundation of China (No. 61308084), the Natural Science Foundation of Shanghai (No. 15ZR1444800),

and the Youth Innovation Promotion Association of the Chinese Academy of Sciences.

## References

- J. Geng, Q. Wang, Y. W. Lee, and S. Jiang, *IEEE J. Sel. Top. Quantum Electron.* **20**, 0904011 (2014).
- K. Scholle, S. Lamrini, P. Koopmann, and P. Fuhrberg, "2  $\mu\text{m}$  laser sources and their possible applications," in *Frontiers in Guided Wave Optics and Optoelectronics*, B. Pal, (eds.) (Intech, 2010), pp. 471.
- K. Yin, B. Zhang, L. Li, T. Jiang, X. Zhou, and J. Hou, *Photon. Res.* **3**, 72 (2015).
- P. Zhang, W. Ma, T. Wang, Q. Jia, and C. Wan, *Chin. Opt. Lett.* **12**, 111403 (2014).
- X. Wang, P. Zhou, X. Wang, H. Xiao, and Z. Liu, *Photon. Res.* **2**, 172 (2014).
- J. Wu, S. Jiang, T. Luo, J. Geng, N. Peyghambarian, and N. P. Barnes, *IEEE Photon. Technol. Lett.* **18**, 334 (2006).
- B. M. Walsh, N. P. Barnes, D. J. Reichle, and S. Jiang, *J. Non-Cryst. Solids* **352**, 5344 (2006).
- B. Richards, Y. Tsang, D. Binks, J. Lousteau, and A. Jha, *Opt. Lett.* **33**, 402 (2008).
- F. Huang, X. Liu, W. Li, L. Hu, and D. Chen, *Chin. Opt. Lett.* **12**, 051601 (2014).
- J. Wu, Z. Yao, J. Zong, and S. Jiang, *Opt. Lett.* **32**, 638 (2007).
- S. Gao, P.-W. Kuan, X. Liu, D. Chen, M. Liao, and L. Hu, *IEEE Photon. Technol. Lett.* **27**, 1702 (2015).
- X. Wen, G. Tang, J. Wang, X. Chen, Q. Qian, and Z. Yang, *Opt. Express* **23**, 7722 (2015).
- S. J. L. Ribeiro, J. Dexpert-Ghys, B. Piriou, and V. R. Mastelaro, *J. Non-Cryst. Solids* **159**, 213 (1993).
- R. Balda, J. Fernández, M. A. Arriandiaga, L. M. Lacha, and J. M. Fernández-Navarro, *Opt. Mater.* **28**, 1253 (2006).
- H. T. Munasinghe, A. Winterstein-Beckmann, C. Schiele, D. Manzani, L. Wondraczek, S. Afshar V, T. M. Monro, and H. Ebendorff-Heidepriem, *Opt. Mater. Express* **3**, 1488 (2013).
- J. R. Lincoln, C. J. Mackechnie, J. Wang, W. S. Brocklesby, R. S. Deol, A. Pearson, D. C. Hanna, and D. N. Payne, *Electron. Lett.* **28**, 1021 (1992).
- X. Fan, P. Kuan, K. Li, L. Zhang, W. Li, and L. Hu, *Laser Phys.* **24**, 085107 (2014).
- T. Xue, L. Zhang, L. Wen, M. Liao, and L. Hu, *Chin. Opt. Lett.* **13**, 081602 (2015).
- M. Peng, C. Wang, D. Chen, J. Qiu, X. Jiang, and C. Zhu, *J. Non-Cryst. Solids* **351**, 2388 (2005).
- Y.-W. Lee, H.-Y. Ling, Y.-H. Lin, and S. Jiang, *Opt. Mater. Express* **5**, 549 (2015).
- J. L. Doualan, S. Girard, H. Haquin, J. L. Adam, and J. Montagne, *Opt. Mater.* **24**, 563 (2003).
- D. Creedon, B. R. Johnson, S. D. Setzler, and E. P. Chicklis, *Opt. Lett.* **39**, 470 (2014).
- E. Ji, Q. Liu, Z. Hu, P. Yan, and M. Gong, *Chin. Opt. Lett.* **13**, 121402 (2015).
- J. Boguslawski, J. Sotor, G. Sobon, R. Kozinski, K. Librant, M. Aksienionek, L. Lipinska, and K. M. Abramski, *Photon. Res.* **3**, 119 (2015).
- J. Wang, J. R. Lincoln, W. S. Brocklesby, R. S. Deol, C. J. Mackechnie, A. Pearson, A. C. Tropper, D. C. Hanna, and D. N. Payne, *J. Appl. Phys.* **73**, 8066 (1993).